Self-Association of the Histidine Kinase CheA as Studied by Pulsed Dipolar ESR Spectroscopy

Jaya Bhatnagar,[†‡] Ria Sircar,[‡] Peter P. Borbat,[†‡] Jack H. Freed,[†‡*] and Brian R. Crane[‡*]
[†]Advanced Center for ESR Studies (ACERT) and [‡]Department of Chemistry and Chemical Biology, Cornell University, Ithaca, New York

ABSTRACT Biologically important protein complexes often involve molecular interactions that are low affinity or transient. We apply pulsed dipolar electron spin resonance spectroscopy and site-directed spin labeling in what to our knowledge is a new approach to study aggregation and to identify regions on protein surfaces that participate in weak, but specific molecular interactions. As a test case, we have probed the self-association of the chemotaxis kinase CheA, which forms signaling clusters with chemoreceptors and the coupling protein CheW at the poles of bacterial cells. By measuring the intermolecular dipolar interactions sensed by spin-labels distributed over the protein surface, we show that the soluble CheA kinase aggregates to a small extent through interactions mediated by its regulatory (P5) domain. Direct dipolar distance measurements confirm that a hydrophobic surface at the periphery of P5 subdomain 2 associates CheA dimers in solution. This result is further supported by differential disulfide cross-linking from engineered cysteine reporter sites. We suggest that the periphery of P5 is an interaction site on CheA for other similar hydrophobic surfaces and plays an important role in structuring the signaling particle.

INTRODUCTION

Bacteria sense and respond to changes in their environment through a sensory apparatus that primarily comprises transmembrane chemoreceptors, the histidine kinase CheA, and the coupling protein CheW (1,2). Cellular studies in *Escherichia coli* as well as in other bacteria have shown that these proteins are organized into higher-order assemblies or clusters at the poles of the cell (2–8). Recent electron cryotomography of these clusters reveal them to form a hexagonal lattice on the cytoplasmic side of the membrane, in which the long, rod-shaped receptors project down from the membrane to associate a layer of CheA and CheW at their tips (6,7,9,10). These structures generate the high sensitivity, gain, and dynamic range exhibited by the chemotaxis system. The hexagonal lattice of the receptors viewed by electron cryotomography is consistent with a basic unit composed of a trimer-of-receptor dimers (7,9–17), but the arrangement of CheA and CheW within the ternary complex is not well understood.

The histidine kinase CheA is a homodimer, with each subunit consisting of five distinct functional domains, from P1 to P5. P1 contains the histidine that is the site of autophosphorylation, P2 docks CheY (the phosphocarrier protein that receives phosphate from P1), P3 dimerizes CheA, P4 (the kinase domain) binds ATP, and P5 (the regulatory domain) couples CheA to CheW and receptors. Whereas P3, P4, and P5 are closely linked and form a somewhat rigid assembly referred to as CheAΔ289 (18), the substrate-binding domain (P1) and CheY-docking domain (P2) are joined to each other and to CheAΔ289 through long variable linkers that provide high mobility (19–21). The regulatory domain P5 and CheW are structurally similar, each made of two intertwined SH3-like β-barrel domains, designated as subdomain 1 and 2. The end of each β-barrel in both CheW and P5 domain contains conserved, exposed, hydrophobic residues (18). CheW binds CheA in a pseudosymmetric interaction with the hydrophobic end of P5 subdomain 1 interacting with the hydrophobic end of CheW subdomain 2 (19). In vivo florescence microscopy studies reveal that receptors aggregate via their cytoplasmic domains and that CheW and selected domains of CheA enhance clustering (5). Thus, one might expect that CheA and CheW associate into an extended structure that binds the receptors and bridges them to each other.

CheA monomers have been suggested to play a major role in propagating conformational changes not only within the homo-dimer, but also to monomer units of nearby CheA dimers (22). In crystal structures of CheAΔ289 alone (18) and in complex of CheAΔ354 (P4P5) with CheW (19), subdomain 2 of P5 makes a symmetric interaction with a neighboring P5 domain in a manner that closely mimics the contact between CheW and the P5 subdomain 1 (Fig. 1). Notably, residues in this region are conserved among CheA sequences (18,23) and mutations of residues near or at this surface affect the ability of chemoattractants to modulate kinase activity (24). Also, the failure to resolve NMR resonances from CheAΔ289 was partly attributed to transient associations between different dimers (25). Based on these observations, we proposed that a P5-P5 contact may have a functional role (19).

Numerous biophysical and biochemical methods have been developed to probe macromolecular associations and many have been applied to the chemotaxis system. These techniques generally fall into two categories: 1), those that

Submitted December 9, 2011, and accepted for publication March 12, 2012.
*Correspondence: jhf3@cornell.edu or bc69@cornell.edu
Editor: David Cafiso.

0006-3495/12/05/2192/10 $2.00
doi: 10.1016/j.bpj.2012.03.038

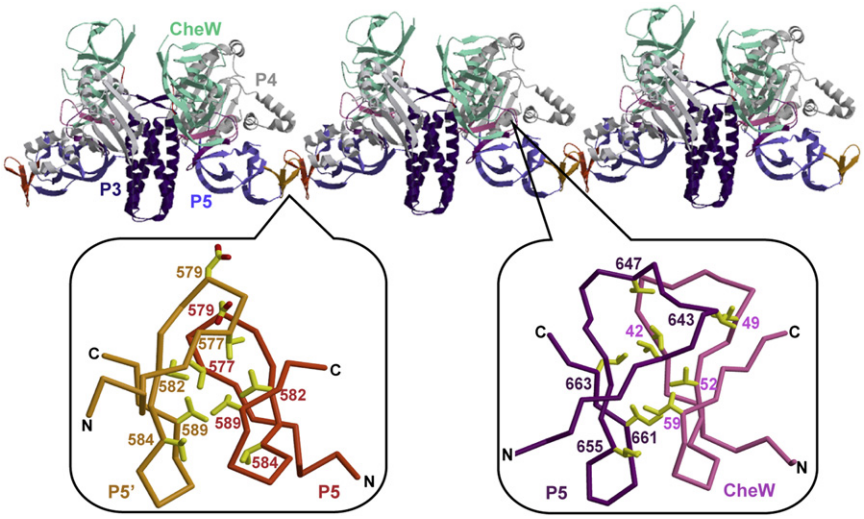

FIGURE 1 Interfaces that mediate CheA to CheA and CheA to CheW contacts in crystals. In crystal structures, a symmetric contact between the P5 domains mediates dimer associations. ESR structures of the complex between CheA (P3, *dark-blue ribbons*; P4, *gray ribbons*; P5, *light-blue ribbons*) and CheW (*green*) are shown associated through the P5-P5 interface found in crystal contacts. (*Insets*) Interfaces formed between CheW and P5 subdomain 1 (*purple* and *magenta ribbons*) and between the two P5 domains (*orange* and *red ribbons*) have similar hydrophobic character.

directly monitor residue proximity on the binding partners (19,26,27), and 2), those that rely on competition between specific modification sites and the binding interaction (21,28–30). Both approaches are most effective when the interface of interest is highly represented within the sample. However, some associations may be destabilized in purified or reconstituted systems due to the lack of accessory factors, cellular localization, or chemical modifications otherwise present in vivo. Nevertheless, characterization of these weakened or minority interactions could prove instructive for understanding cellular function. As a test case, we have probed the association properties of *Thermotoga maritima* CheA in solution by what to our knowledge is a new application of pulsed dipolar electron spin resonance (ESR) spectroscopy (31–34) and then we have verified interacting surfaces by cross-linking studies. Dimers of CheAΔ289 do self-associate in solution, and the interface involved is either the same or closely related to the one that participates in the aforementioned crystal contacts of subdomain 2. Furthermore, CheW does not appear to affect self-association of dimeric CheA.

MATERIALS AND METHODS

Characterization of protein association/aggregation by pulsed dipolar electron spin resonance (ESR) spectroscopy

The dipolar coupling $A(\mathbf{r})$ between spins A and B separated by vector $\mathbf{r} = (r,\theta)$, with θ the angle between $\mathbf{r}$ and the direction of the external magnetic field, $\mathbf{B}_0$, is given in angular frequency units by

$$A(\mathbf{r}) = \omega_d\left(1 - 3\cos^2\theta\right). \quad (1)$$

Here,

$$\omega_d = 2\pi\nu_{dip} = \frac{\mu_0\gamma_e^2\hbar}{4\pi r^3}$$

is the dipolar constant, γ_e is the gyromagnetic ratio of electron spin, and $\hbar$ is Planck's constant divided by 2π. Note that $A(\mathbf{r})$ produces oscillations in the time-dependent ESR signals and can be isolated with a proper pulse sequence (19,31,34,35). In isotropic solutions, this dipolar evolution is a function of ω_d, i.e., just of r.

Pulsed double electron-electron resonance (DEER or PELDOR) effectively resolves dipolar coupling with distances ≥ 20 Å through a spin-echo technique (31–33,35,36). Compared to the alternative method of double quantum coherence (34,37), DEER provides easier referencing of the dipolar signal amplitude, which can be used to obtain information about the homogeneity of the spin-labeled protein distribution throughout the sample. The spin-echo amplitude from an isolated pair of spins in DEER (31,32,38) can be written as

$$\begin{aligned} V_{intra}(t) &= \left\langle V_0(\mathbf{r}/r)\left[1 - 2\ p\sin^2\left(\frac{1}{2}A(\mathbf{r})t\right)\right]\right\rangle_{\mathbf{r}} \\ &\cong V_0\left(1 - p + p\langle\cos(A(\mathbf{r})t)\rangle_{\mathbf{r}}\right), \end{aligned} \quad (2)$$

where p represents the fraction of spins flipped by the pump pulse. The angle brackets denote averaging over all possible $\mathbf{r}$ values. The average over $\mathbf{r}$ in Eq. 2 is simplified by assuming no orientation selection (39), which usually holds well for flexible tether MTS spin labels. Note also that $V_{intra}(t)$ in DEER contains a large contribution from spin pairs not affected by the pump pulse, $V_0(1-p)$.

The amplitude of the DEER time-domain signal, $V(t)$, can be factored into an intramolecular contribution, V_{intra} (Eq. 2), which gives the dipolar interaction in a pair of sufficiently isolated spatially correlated spins (i.e., on the same molecule), and a nonspecific intermolecular contribution, V_{inter}, from the dipolar interaction with the spins randomly located within a few hundred Ångstroms from the spins of the pair (32),

$$V(t) = V_{intra}(t)V_{inter}(t). \quad (3)$$

V_{inter} is a monotonically decaying signal that modifies V_{intra}, and thereby gives rise to a large background (baseline) signal. For an N spin system, e.g., for a spin-labeled oligomer of order N, bearing nitroxide spins $k = 1, \ldots, N$, the dipolar signal in DEER can be written as a product according to Milov et al. (38) as

$$V_{intra}(t) = V_0N^{-1}\left\langle\sum_{i=1}^{N}\prod_{k\neq i}[1 - p_{ik}u_{ik}(\mathbf{r}_{ik},t)]\right\rangle_{\mathbf{r}_{ik}}. \quad (4)$$

Here,

$$u_{ik}(\mathbf{r}_{ik},t)\equiv\langle 1-\cos(A(\mathbf{r}_{ik})t)\rangle_{\mathbf{r}_{ik}}$$

is the dipolar signal detected on spin i when pumping on spin k, p_{ik} is the probability of flipping spin k by the pump pulse, and $\mathbf{r}_{ik}$ is the vector connecting spins i and k. Equation 4 can be reduced to the form of Eq. 3 by Markoff configurational averaging (40) over the spin distribution throughout the sample. Protein solutions can generate an isotropic but not necessarily uniform spin distribution because of spatial correlations through excluded volume (41) or interaction effects (42). In this case, one finds by using the Markoff method,

$$V_{\text{inter}}(t)=\exp\left\{-k_0p\overline{C}t-9\sqrt{3}k_0p\overline{C}\int_0^\infty f(r)r^2dr\times\int_0^1 dx\,\sin^2\left[\frac{1}{2}\omega_d t\left(1-3x^2\right)\right]\right\},\tag{5}$$

where

$$k_0=\frac{2\pi\mu_0\gamma_e^2\hbar}{9\sqrt{3}}\approx 10^{-3}\mu M^{-1}\mu s^{-1},$$

$\overline{C}$ is the average spin concentration over the sample, and $f(r)\equiv 1-C(r)/\overline{C}$ represents the effect of local spin concentration, $C(r)$, in heterogeneous samples. For uniform spin distribution when $C(r)=\overline{C}$ $f(r)=0$, Eq. 5 reduces to a well-known form $V_{inter}=\exp(-pk_0Ct)$. If one approximates $C(r)$ by a constant local concentration, C_{loc}, then

$$V_{inter}\cong\exp(-pk_0C_{loc}t).\tag{6}$$

pC_{loc} thus can be estimated from the slope of the baseline in the logarithmic plot of $V(t)$ (compare to Eq. 2), i.e., from log $V_{inter}(t)$. Because p can be obtained with adequate accuracy computationally or from experiments with a suitable reference sample, C_{loc} can be estimated. Thus, aggregation, which strictly should be analyzed based on Eq. 4, can often be approximated by introducing an equivalent local spin concentration. Note that large deviation of C_{loc} from constant value, such as those due to steric constraints or other interactions, will cause small deviations from linearity in log $V_{inter}(t)$, especially for early time points. For this reason, V_{intra} is sometimes extracted from a total signal using a baseline fit to a second or a higher degree polynomial. Finally, we note, that the contribution to the dipolar signal from electron spins separated by a distance r, large enough to satisfy (i.e., $r\geq 65$ Å for t_m 3 μs), falls with r as $(\gamma_e^2\hbar t_m/r^3)^2$. For $r=150$ Å and $t_m=3$ μs, this gives only ~0.08 of the maximal dipolar signal. Consequently, in an aggregate, the contribution of surrounding spins beyond the radius $R_{max}\cong(\gamma_e^2\hbar t_m)^{1/3}$ falls as $1/r^3$, so the local spins beyond ~150 Å contribute negligibly to the DEER signal.

Pulsed ESR measurements

Double electron-electron resonance (DEER) experiments were carried out at 17.35 GHz on a home-built 2D-FT ESR spectrometer, with either 16-ns or 32-ns pump pulses (19,43). When measuring signals in protein complexes, the proteins were mixed together and the sample incubated at room temperature for 30–60 min before freezing for the ESR experiments. Protein concentrations used for DEER experiments were typically in the range of 25–50 μM, unless as noted. The baseline was approximated by a linear polynomial in most cases. Subsequently, distance distributions were calculated by Tikhonov regularization (44) and further refined by a maximum entropy regularization method (45).

Magnetic dilution experiments were performed by keeping the protein spin concentration constant while increasing the concentration of unlabeled, wild-type, i.e., Cys-less CheAΔ289. Unlabeled protein was added in three and five times' excess of concentration of spin-labeled protein (usually at 25 μM).

Protein expression and purification

Genes encoding CheAΔ289 (P3-P4-P5 domain, 290–671), P4P5 (355–671), CheW (1–151), and cytoplasmic domain (residues 40–213) of *T. maritima* receptor TM0014 were PCR-cloned into the vector pET28a (Novagen, Madison, WI), and the proteins expressed with an N-terminal His_6 tag and purified by Ni-NTA affinity chromatography and size-exclusion chromatography as described previously (18,46).

Site-directed mutagenesis and spin labeling

In a cysteine-less background of CheAΔ289, seven residues (Q545, N553, S568, D579, E646, D634, and S639) in P5 domain and an equal number in P4 domain (D371, E387, E401, K458, K496, D508, and S522) and one residue D579 in CheAΔ354 (P4P5) were separately changed to cysteines by Quik-Change mutagenesis (Stratagene, LaJolla, CA). These proteins were spin-labeled with (1-oxyl-2, 2, 5, 5-tetramethylpyrolinly-3-methyl)-methanethiosulfonate with the procedure described previously (19).

Cross-linking experiments

The stock solution of the initiator Cu(II)(1,10 phenanthroline)$_3$ was prepared according to the procedure of Bass et al. (47). For each reaction, the final reaction volume was kept constant at 15 μl, which included 5 μl of NuPAGE LDS sample dye (Invitrogen, Carlsbad, CA). All the proteins were solubilized in gel filtration buffer (50 mM TRIS, pH 7.5 and 1 mM NaCl). The final concentration of cysteine-substituted CheAΔ289 proteins varied between 1 and 2 μM in the final reaction mixture, whereas the initiator concentration was fixed to 0.1 mM in all cases. A quantity of 10 μl of the reaction mixture was loaded on sodium dodecyl-sulphate polyacrylamide gel electrophoresis (SDS PAGE) gel for analysis by Coomassie staining.

RESULTS

Size-exclusion chromatography indicates that CheA dimers associate in tetramers

CheA kinases are predominantly dimers in solution (48–50). Nevertheless, *T. maritima* CheA and CheAΔ289 (P3-P4-P5) forms higher state oligomers in solution. The elution profile from gel filtration chromatography (Superdex 200 column; GE Life Sciences, Little Chalfont, United Kingdom) of wild-type CheAΔ289 shows a dimer as the majority species (molecular mass 84 kDa), along with a small population of higher state oligomers (Fig. 2). These oligomers are likely to be tetramers (dimer of dimers) because of their elution volume and the fact that cross-linked CheA dimers elute at the same position. Along with the wild-type protein, ~20 cysteine (Cys) substitution variants of CheAΔ289 also show tetramer formation, both with and without covalent cross-linking (data not shown). For some preparations, a small fraction of the protein formed even larger aggregates and eluted in the void volume of the column.

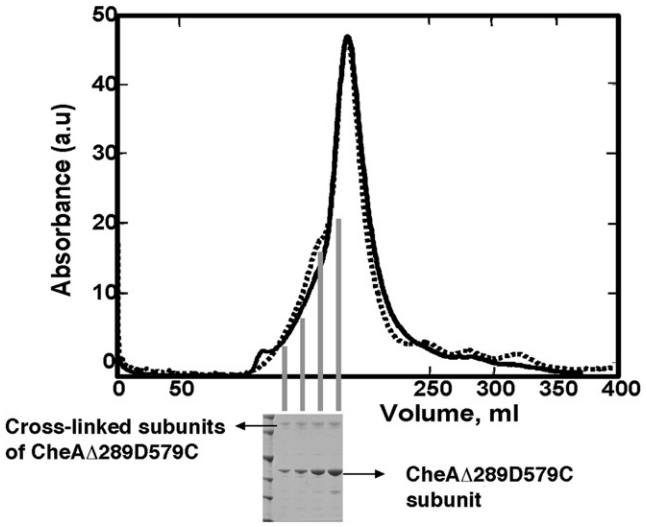

FIGURE 2 Minor CheA aggregation evident from size-exclusion chromatography. Overlay of gel filtration profiles of wild-type CheAΔ289 (*solid line*) and CheAΔ289 D579C (*dotted line*) show the dominant elution peak corresponds to the molecular mass of dimer, whereas a small shoulder at 163 ml indicates higher-order associations. The SDS PAGE analysis of selected fractions close to the peak shoulder from CheAΔ289 variant D579C (*below*) produces higher molecular-mass bands (~84 kDa), which correspond to the two cross-linked monomer subunits of CheAΔ289D579C from two different dimers.

DEER experiments

Nonspecific dipolar signals from spin-labeled CheAΔ289

The DEER signal, $V(t)$, which reflects both the frequency and strength (amplitude) of the dipolar interaction, can be well approximated by a product of intramolecular (V_{intra}) and intermolecular (V_{inter}) dipolar contributions (Eq. 3). In a homogenous protein solution, the intermolecular contribution leads to a simple exponential decay from which the local spin concentration can be calculated (Eq. 5). This decay modifies both the signal of interest (i.e., V_{intra}) and the constant background. The latter now appears as a monotonically decaying baseline. The logarithm of the signal amplitude, plotted versus time, produces a line with a slope k that is proportional to local protein concentration; spins at distances greater than a few hundred Ångstroms do not contribute to the signal. In pulsed dipolar electron spin resonance (ESR) spectroscopy experiments, conducted on several spin-labeled Cys variants of CheAΔ289, we consistently observed that the apparent spin concentration calculated from a DEER experiment (Eq. 5) was a factor of 4–5 higher than that expected based on protein concentration.

This apparent increase in local concentration points to the possibility of small-scale aggregation. In such a case, the local spin concentration within a radius of 15–100 Å from a given spin pair is greater than the average spin concentration throughout the sample and thereby increases the slope of $\ln(V(t))$ versus time compared to that expected for the average (bulk) concentration. To confirm the presence of aggregates, we performed magnetic dilution experiments by progressively increasing fractions of Cys-less protein, in the presence of unchanged concentrations of spin-labeled protein. This has the effect of reducing the local spin-labeled protein concentration because unlabeled proteins replace (some of) them, whereas the average concentration of spin-labeled protein is unaffected. In other words, the unlabeled molecules replace those with spin-labels while keeping the average spin concentration constant. At sufficiently high levels of magnetic dilution, the local spin concentration will decrease, but the contribution from the random spin distribution remains unchanged. Thus, the spin distribution, as sensed by a localized spin-pair, becomes more uniform. When the normalized signals from successively diluted samples are compared to each other, a reduction in the slope indicates the presence of association/aggregation.

Magnetic dilution experiments with spin-labeled sites on all three domains of CheAΔ289 confirmed the presence of higher order associations of CheA in solution, but notably the behavior varied with spin-label position (Fig. 3). In particular, magnetic dilution reduced intermolecular signals from spin labels on P4 (Fig. 4 *a*) and those sites which are located at the peripheral end of the P5 domains (Fig. 4 *b*). In contrast, spins located close to or on the P3 domain showed nearly no multispin effects (Fig. 4, *c* and *d*). Although these data do not allow us to propose the structure of the aggregate(s), they suggest, given the size and structure of CheA (Fig. 3), that the dimers are associating via the surfaces of P4 and P5 that are distal to P3. In the

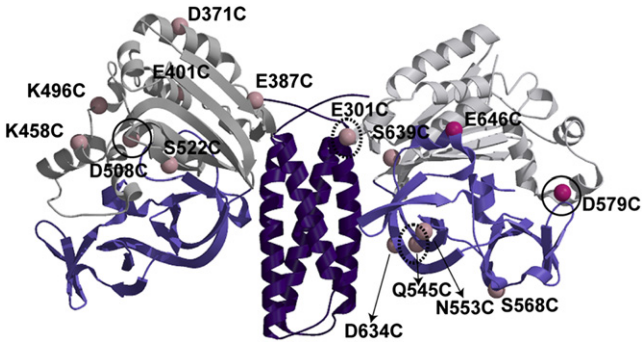

FIGURE 3 Spin-label positions on the CheAΔ289. Position of spin-label sites on the crystal structure of CheAΔ289 that were tested in cross-linking and magnetic dilution experiments. Sites on the P4 and P5 domain used for cross-linking experiments (*spheres*) are shown on different subunits. From a set of 14 sites, only E646C and D579C on P5 domain (*dark-pink spheres*) were found to form disulphide bonds readily. Magnetic dilution experiments were performed with four spin-labeled sites (E301C, Q545C, D508C, and D579C) on CheAΔ289. Sites D508C and D579C (*spheres* marked with *solid black circles*) are located at the periphery of the complex and show drastic reduction in baseline slope when unlabeled CheAΔ289 protein is added. In contrast, only minor changes were observed for E301C and Q545C (*spheres* marked with *dashed black circle*), as they are located near the core of the protein.

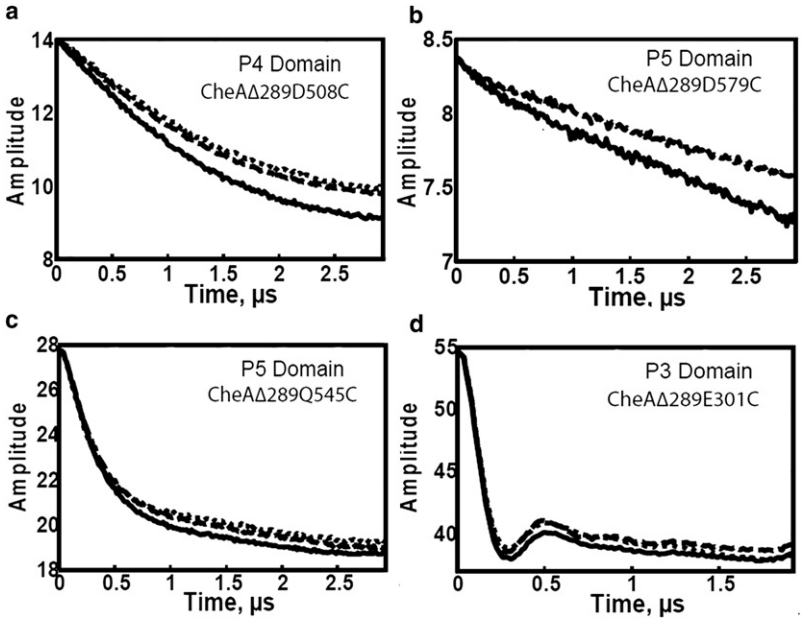

FIGURE 4 Magnetic dilution experiments on spin-labeled CheA. Magnetic dilution experiments were carried out with four (E301C, D508C, Q545C, and D579C) spin-labeled sites on CheAΔ289. Whereas the first two sites belong to domain P3 and P4, respectively, the latter two are located on different ends of P5 domain. In all samples, the concentration of spin-labeled protein was kept constant at 25 μM. The solid line in each plot shows the DEER signal obtained from spin-labeled CheAΔ289 without dilution. Wild-type protein was added in three (*dashed line*) and five times (*dotted line*) concentration excess of spin-labeled CheAΔ289. Stoichiometric amounts of wild-type CheW were added in all samples.

aggregates, the P3 domains, which reside at the center of the dimers, must be separated by ~100 Å or more to provide only a small contribution to the aggregation effects. (Note that there is also a distinct intramolecular signal from the symmetric spins across the P3 domain within one dimer, as evidenced by the strong oscillatory shape of Fig. S1 in the Supporting Material.)

Specific intermolecular dipolar signals from spin-labeled CheAΔ289

We have measured dipolar distances between several spin-labeled sites on CheAΔ289. With the exception of D579C in P5 domain, the dipolar signals from all the Cys-substituted CheAΔ289 variants gave average distances of separation that agree well with the intramolecular distances measured between the C_β coordinates of the native residues in the crystal structure of CheAΔ289 dimer (see Table S1 in the Supporting Material). However, with D579C, in addition to a very long distance that cannot be measured directly but is consistent with the 103 Å separation of these symmetric sites within the dimer, we observed a weak dipolar signal representing a much shorter distance (compare to Fig. 5). Residue 579 is located at the peripheral end of the P5 domain (subdomain 2), hence the presence of this additional short distance argues in favor of two CheA dimers associated via an interface that brings the two 579 positions close together.

The short distance component increased from 15 to 30% of maximum dipolar signal amplitude when the protein concentration was changed from 50 to 100 μM, which would be expected for a bimolecular association, but further increase in the concentration of spin-labeled CheAΔ289D579C failed to increase the short distance component. At such high protein concentrations, other modes of nonspecific association may compete with the specific association through the P5 domains. However, increase in protein concentration to 500 μM along with reduction of the cryoprotectant glycerol in the ESR sample from 30 to 10% also increased the association and resulted in strong dipolar signals with R_{avg} of $<$20 Å (Fig. 5). In the presence of CheW, the short distance signal persisted from the 579 site, but due to the weak nature of the signal, it could not be determined whether CheW promotes or prevents self-association. We also observed a signal from P5 site 646 consistent with a short distance component, but the distributed nature of the DEER signal prevented assignment of a specific short distance (Fig. 5).

We further investigated whether the CheA aggregation as reported by the 579 site depended on the CheA dimerization domain by generating a fragment of CheA composed of only the P4 and P5 domains (P4P5) and spin-labeling at position 579. P4P5 at 10% glycerol concentration gave a comparable, short distance dipolar signal as CheAΔ289, with no contribution from the very long distributed distance (Fig. 5). Under slow freezing conditions, as implemented here, 10% glycerol reduces solvent vitrification and thereby increases effective protein concentration (51). The short distance component for P4P5 increased from 11 to 25% of maximum dipolar signal amplitude when the protein concentration was changed from 50 to 500 μM and the glycerol concentration reduced. Thus, CheA self-association is likely mediated by the P5 domain and does not require CheA dimerization. Unfortunately, the P5 domain was not stable when expressed alone and thus could not be tested for aggregation.

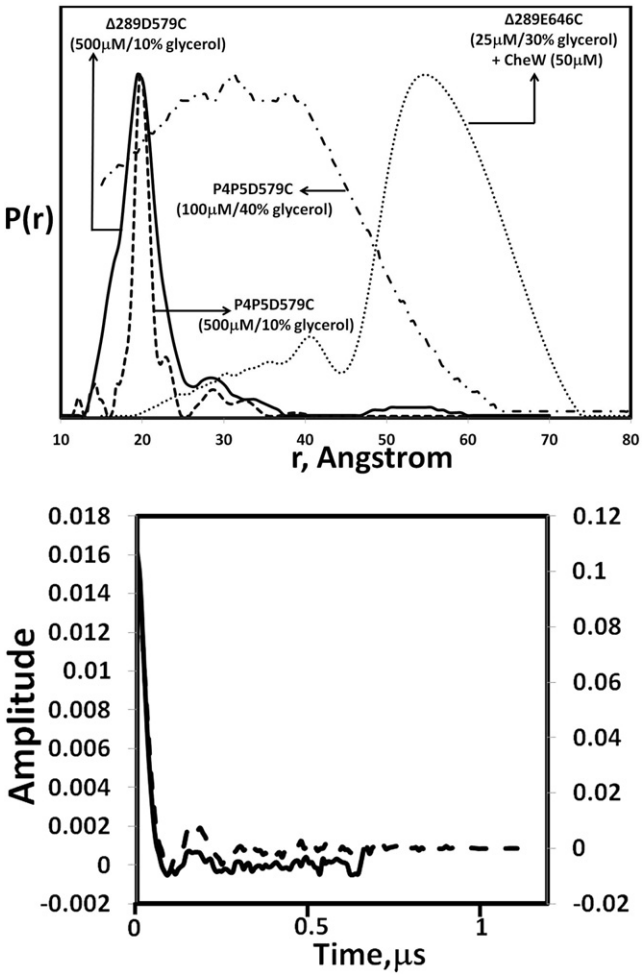

FIGURE 5 Distance distributions for spin-labels at the 579 position. Short reconstructed distances of spin-label separation in both CheAΔ289-D579C (500 μM, 10% Gly; *solid line*) and P4P5-D579C (500 μM, 10% Gly; *dashed line*) are consistent with intermolecular interactions between P5 subdomain 2. Corresponding time domain spectra shown in the panel below. For comparison, the highly distributed signal of P4P5-D579CP4P5 is shown at lower protein and higher glycerol concentration (100 μM, 40% Gly; *dash-dotted line*). The distribution of for CheAΔ289-D646C is dominated by the broad, intradimer distance at ~60 Å, but also shows some features in the short distance range (25 μM; CheW, 50 μM, 30% Gly; dotted line). CheW was added to block self-associations and cross-linking through subdomain 1 (see Fig. 6). For ease of comparison, the heights of the distance distributions are scaled to 1.

Cross-linking experiments

CheA without CheW

Site-directed disulphide cross-linking is a useful method to determine residue proximity at the interface of a protein complex (47). In the absence of nonspecific interactions, only those cysteine pairs on the interface that have their β-centers separated by 4–8 Å readily form disulphide bonds (cross-link) with ambient or supplied oxidizing agents. With several cysteine variants of CheAΔ289 in hand, we applied this strategy to confirm if P5 subdomain 2 is indeed involved in self-association of CheAΔ289. We tested 14 variants of CheAΔ289 for their ability to cross-link. The cysteine substitutions were evenly divided between P4 and P5 domains and were uniformly distributed over the surface of domains (Fig. 3). Whereas all of the cysteine substitutions on P4 domain gave negative results, two positions on the P5 domain readily formed cross-links: E646C and D579C (Fig. 6). In both cases, increased cross-linking with increased protein concentration indicated that the 646 and 579 disulfide bonds were forming between dimers and not between subunits.

Effect of CheW and receptor fragments on cross-linking

The autophosphorylation activity of kinase CheA is regulated by CheW and chemoreceptors (52,53). Receptor cluster formation depends upon CheA and CheW (5). CheA cross-linking at E646C was prevented by CheW. In contrast, CheW did not reduce cross-linking at D579C. These results are consistent with CheW binding to subdomain 1 of CheA P5, and blocking access to position 646. The presence of an unlabeled receptor cytoplasmic signaling domain that is known to inhibit *T. maritima* CheA (46) did not affect cross-linking at either the 646 or 579 site, irrespective of the presence or absence of CheW.

DISCUSSION

We have applied pulsed dipolar electron spin resonance (ESR) spectroscopy to probe the aggregation properties of the histidine kinase CheA. Previously, this technique has

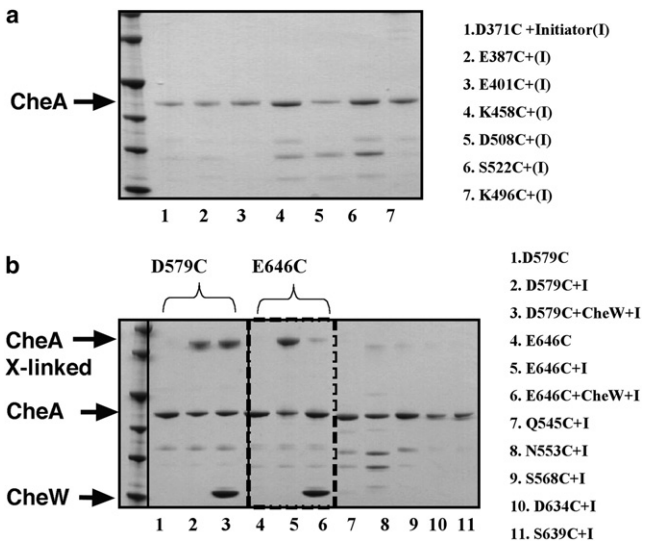

FIGURE 6 CheA cross-linking. Fourteen cysteine-substituted variants of CheAΔ289 were tested for their ability to form disulphide bonds or cross-link in presence of an oxidizing reagent. (*a*) None of the seven cysteine substitutions on P4 domain successfully cross-linked. (*b*) Out of seven positions on P5 domain, D579C and E646C (lanes *2* and *5*, respectively) cross-linked. Disulfide formation by E646C was blocked by CheW (lane *6*) whereas that by D579C was unaffected (lane *3*).

been applied to higher oligomeric states only in the study of model polynitroxide radicals (54), clusters formed by organic radicals in small peptides (31,55), and (only recently) to small-size proteins (~15 kDa) (56). In most of these small systems, aggregation properties were derived from a measured distance or amplitude of the dipolar signal rather than by monitoring changes in baseline produced by the addition of an unlabeled component, as we have done in magnetic dilution studies of CheAΔ289 performed as of this article's writing. In aggregates formed by doubly spin-labeled proteins, both the intermolecular and intramolecular spin distances are typically within the pulsed dipolar ESR spectroscopy range (31). Sites located on the outer protein surface will experience different local concentrations of surrounding spins on other proteins as compared to those located inside the protein and hence will respond to magnetic dilution differently (compare to Materials and Methods). Here, for the first time to our knowledge, we have applied baseline analysis to test aggregation states of high-molecular mass molecules (>50 kDa). As an added advantage, we demonstrate that this method can also identify the protein regions and surfaces that participate in aggregation.

Chemotaxis proteins CheA and CheW and receptors interact closely and form compact clusters at the poles of the cell (14–16,19,28). Clearly, clustering could be critical for signal processing and amplification as it provides a potential mechanism for the high degree of cooperativity that connects kinase response to ligand binding (2,8). CheA and CheW may not just play a role in controlling how the receptors interact, but they may also act as signal propagators within the dense assembly. Self-association of CheA or CheW could well be an important element of the architecture of the signaling particle and may be subject to change during signal propagation.

The large size and dimeric nature of CheAΔ289 results in strong intramolecular dipolar signals at long distances that have the potential to mask weaker signals between molecules in aggregates. For these reasons, detection of aggregation from spin-pair distance analysis can be challenging. The alternative is to compare the base-line behavior for different sites on the protein surface under the condition of magnetic dilution.

The dipolar signal between two coupled spins superimposes on a baseline that is a contribution from the average local concentration of spins in the sample, which for a homogenous solution is close to the bulk concentration (compare to Materials and Methods). For some sites on CheAΔ289, this number is considerably greater than that for bulk spin concentration in the sample. (In protonated solvents, dipolar signals between spin labels separated by as far as 50–60 Å (31) can be accurately measured by DEER with the upper range usually achieved by solvent deuteration. In the case of typical relaxation times—approximately a few microseconds—spin-labels separated by >~75 Å generally only increase the magnitude of the baseline slope in DEER.) In cases where large spin separations result from aggregation, multiple conformations of the aggregate can cause the spins to be distributed over a range of space large enough to be viewed as a local spin concentration, which will differ from that of the bulk. If excess unlabeled CheAΔ289 is added to the sample, the total sample spin distribution becomes more uniform as the unlabeled dimers replace their spin-labeled counterparts within the aggregates. This is likely the case for spin-labeled sites D508C and D579C, which are located on P4 and P5 domains, respectively (Fig. 4, *a* and *b*). In contrast, we observed only minor changes in the baseline for spin labels at P3 domain (E301C) or those on P5 domain that were located close to P3 domain (Q545C; Fig. 4, *c* and *d*). Thus, these positions sense aggregated spins to a lesser degree than labels residing in P4 or P5. In other words, association through the peripheral surfaces of the P4 and P5 domains holds the P3 domains relatively far apart in the aggregates.

In the absence of a rigorous theory for dipolar signals from aggregates of large proteins, only an estimate of an aggregation number for this system can be given. To begin, we note that only spins within a limited range of distances contribute significantly to the intermolecular dipolar signal (compare to Materials and Methods). Therefore, given the large size of CheA, only one layer of bound molecules (i.e., ~12 nearest neighbors) should be considered in making estimates. Close-packing of CheA within this layer produces a local spin concentration $\leq$20 mM. The value 20 mM is a much higher local concentration than that observed. Application of Eq. 6 under conditions of magnetic dilution shows that the contribution to the base-line slope results from ~0.1 mM spins. Given that the intermolecular distance measurements from site 579 indicate that only ~15–25% of CheA is specifically self-associated (see below), the local concentration within the aggregate is then ~1 mM. This limits the number of molecules in the aggregate to ~2–3. Thus, the proteins likely form small low-order supramolecular assemblies such as dimers or trimers. These oligomeric states may represent linear networks (Fig. 1), such as those found in crystal packing interactions (19). The DEER results emphasize the probable role of P4 and P5 domains in association, thus placing important restrictions on the arrangement of the molecules in the aggregates.

It was reported previously that the hydrophobic region in the subdomain 2 of the P5 domain, which is primarily spanned by β10 and β11 (Fig. 1), mediates contacts with the P5 domain of an adjacent symmetry-related molecule in the crystal lattice of CheAΔ289 (18) as well as in the complex of CheW with CheAΔ354 (19). If indeed CheAΔ289 self-associates through this interface in solution, then it should be possible to detect short distances between spin-labeled sites located very close to this interface.

Because CheAΔ289 is itself a dimer, it becomes challenging to separate the large intramolecular distances (within the dimer) from the intermolecular distances (between self-associated dimers) if both of them are comparable and the affinity of the self-association is low. Conclusions can be drawn only when the two distances are substantially different and can be easily distinguished in the ESR signal. Out of seven cysteine mutations spanning the surface on the P5 regulatory domain, the 579 residue is furthest away from the dimerization domain (P3), which places it in proximity to the hydrophobic surface at one end of P5 domain (Fig. 3).

The intradimer distance measured between the C_β coordinates at this residue in the crystal structure of CheAΔ289 dimer is 103 Å, whereas the interdimer distance calculated by generating the symmetry-related molecules in the crystal is only 8 Å. Thus, if the association between dimers is reasonably populated, the two signals should be distinctly observed in DEER. It should be noted that distances $<$20 Å are not easily detected by DEER (31), but with flexibility of the protein backbone at that site, or motion of the spin label, the separations between nitroxides may become longer and could reasonably fall within the detectable range. With labeled residue 579 on both CheAΔ289 and P4P5, we successfully observed a weak but distinct dipolar signal corresponding to a short distance (within 15–25 Å) along with the expected long intradimer distance from DEER (Fig. 5). It should be noted that the overall effect of aggregation on the DEER signal from all CheA sites is relatively small. Such is the case for D579C, where the short interdimer distance accounts for only ~15% of the signal amplitude expected for all P5 domains.

We applied cross-linking to independently identify specific regions of the P4 and P5 domains that could participate in noncovalent interactions. The advantage of cross-linking studies is that they are relatively easy to implement and they accumulate product, which allows the detection of weak contacts in the sample. A drawback to cross-linking is that a negative outcome does not rule out aggregation, because the tested residues may be too far, positioned improperly, or sufficiently unreactive for cross-linking in the aggregation complex. The sites selected for substitutions with cysteine residues are distributed uniformly over the surface of these domains. The failure of seven sites (E387C, E401C, D71C, K458C, K496C, D508C, and S522C) on P4 to cross-link deemphasizes the role of this domain in specific contacts that promote aggregation. However, we isolated two sites, E646C and D579C on P5, that cross-link readily. In the crystal structure of CheAΔ289 dimer, the two P5 domains are widely separated in space by the dimerization domain. This, along with the concentration dependence of the cross-linking, makes it is highly unlikely that in solution, the P5 domains would move close enough to form intramolecular disulphide bonds. Furthermore, the cross-linking experiments are carried out at concentrations where there is little CheA monomer (50). Also, when mapped onto the structure of the P5 domain, the residues 646 and 579 are sufficiently far apart and close to two distinct hydrophobic regions, one of which has been shown to bind strongly to CheW (19,24,26,27).

The accessibility and mobility of this P5 region should be significantly affected by CheW, which was indeed manifested as a decrease in the cross-linking of E646C in the presence of CheW, whereas no CheW-dependence was observed with D579C. It appears that the hydrophobic ends of P5 subdomain 1 and 2 have a strong tendency to associate with a like surface, whether it be found on another P5 domain or CheW. Thus, in the absence of CheW, both ends of P5 can mediate self-association with another P5, but when CheW is present, its high specificity for subdomain 1 blocks access of another P5 domain. As CheW does not appear to interact with P5 subdomain 2 under these conditions, this domain remains free to mediate dimer-to-dimer contacts. In fluorescence microscopy experiments, CheW and the C-terminal P5 domain were found to promote receptor clustering (5). Given the fact that both protein domains are structurally similar, the hydrophobic surfaces in each of them could well be involved in self-association and hence instrumental in bringing together receptors.

Cysteine-scanning analysis of *E. coli* CheA identified sites close to the P5-P5′ interaction surface where residue substitutions produced kinases that failed to deactivate in the presence of attractant (24). Similarly, three mutants of the P5 domain at the P5-P3 interface isolated as phenotypic suppressors of receptor defects (V606M, G627D, G627C) also failed to deactivate kinase in presence of attractant (24). These studies indicate that changes in the positioning and interaction of the P5 domains are important for kinase regulation. Although the P5-P5′ association is not a high-affinity interaction in solution, the protein concentration in the receptor arrays is likely $>$10 mM (2,6,7,9); in such a constrained environment, weak but specific contacts could construct important structural elements. Our work suggests that the peripheral end of P5 subdomain 2 is a primary site for mediating such contacts. We emphasize that the conserved hydrophobic surfaces at the ends of P5 subdomains 1 and 2 are effective binding sites for like domains. Although the details remain to be worked out, CheW and P5 have the capability to supply important latch points within a higher-order assembly of the signaling particle.

SUPPORTING MATERIAL

Table S1 and Fig. S1 are available at http://www.biophysj.org/biophysj/supplemental/S0006-3495(12)00379-7.

This work was supported by the National Institutes of Health P41RR016242, P41GM103521, and 2R01EB003150 to J.H.F., and GM066775 to B.R.C.).

REFERENCES

1. Wadhams, G. H., and J. P. Armitage. 2004. Making sense of it all: bacterial chemotaxis. *Nat. Rev. Mol. Cell Biol.* 5:1024–1037.
2. Hazelbauer, G. L., J. J. Falke, and J. S. Parkinson. 2008. Bacterial chemoreceptors: high-performance signaling in networked arrays. *Trends Biochem. Sci.* 33:9–19.
3. Maddock, J. R., and L. Shapiro. 1993. Polar location of the chemoreceptor complex in the *Escherichia coli* cell. *Science.* 259: 1717–1723.
4. Sourjik, V., and H. C. Berg. 2000. Localization of components of the chemotaxis machinery of *Escherichia coli* using fluorescent protein fusions. *Mol. Microbiol.* 37:740–751.
5. Kentner, D., and V. Sourjik. 2006. Spatial organization of the bacterial chemotaxis system. *Curr. Opin. Microbiol.* 9:619–624.
6. Zhang, P. J., C. M. Khursigara, …, S. Subramaniam. 2007. Direct visualization of *Escherichia coli* chemotaxis receptor arrays using cryo-electron microscopy. *Proc. Natl. Acad. Sci. USA.* 104:3777–3781.
7. Briegel, A., D. R. Ortega, …, G. J. Jensen. 2009. Universal architecture of bacterial chemoreceptor arrays. *Proc. Natl. Acad. Sci. USA.* 106:17181–17186.
8. Sourjik, V. 2004. Receptor clustering and signal processing in *E. coli* chemotaxis. *Trends Microbiol.* 12:569–576.
9. Briegel, A., H. J. Ding, …, G. J. Jensen. 2008. Location and architecture of the *Caulobacter crescentus* chemoreceptor array. *Mol. Microbiol.* 69:30–41.
10. Khursigara, C. M., X. W. Wu, and S. Subramaniam. 2008. Chemoreceptors in *Caulobacter crescentus*: trimers of receptor dimers in a partially ordered hexagonally packed array. *J. Bacteriol.* 190:6805–6810.
11. Kim, K. K., H. Yokota, and S. H. Kim. 1999. Four-helical-bundle structure of the cytoplasmic domain of a serine chemotaxis receptor. *Nature.* 400:787–792.
12. Lefman, J., P. J. Zhang, …, S. Subramaniam. 2004. Three-dimensional electron microscopic imaging of membrane invaginations in *Escherichia coli* overproducing the chemotaxis receptor Tsr. *J. Bacteriol.* 186:5052–5061.
13. Shrout, A. L., D. J. Montefusco, and R. M. Weis. 2003. Template-directed assembly of receptor signaling complexes. *Biochemistry.* 42:13379–13385.
14. Studdert, C. A., and J. S. Parkinson. 2004. Crosslinking snapshots of bacterial chemoreceptor squads. *Proc. Natl. Acad. Sci. USA.* 101:2117–2122.
15. Studdert, C. A., and J. S. Parkinson. 2005. Insights into the organization and dynamics of bacterial chemoreceptor clusters through in vivo crosslinking studies. *Proc. Natl. Acad. Sci. USA.* 102:15623–15628.
16. Ames, P., C. A. Studdert, …, J. S. Parkinson. 2002. Collaborative signaling by mixed chemoreceptor teams in *Escherichia coli*. *Proc. Natl. Acad. Sci. USA.* 99:7060–7065.
17. Boldog, T., S. Grimme, …, G. L. Hazelbauer. 2006. Nanodisks separate chemoreceptor oligomeric states and reveal their signaling properties. *Proc. Natl. Acad. Sci. USA.* 103:11509–11514.
18. Bilwes, A. M., L. A. Alex, …, M. I. Simon. 1999. Structure of CheA, a signal-transducing histidine kinase. *Cell.* 96:131–141.
19. Park, S. Y., P. P. Borbat, …, B. R. Crane. 2006. Reconstruction of the chemotaxis receptor-kinase assembly. *Nat. Struct. Mol. Biol.* 13:400–407.
20. Morrison, T. B., and J. S. Parkinson. 1994. Liberation of an interaction domain from the phosphotransfer region of CheA, a signaling kinase of *Escherichia coli*. *Proc. Natl. Acad. Sci. USA.* 91:5485–5489.
21. Zhou, H., M. M. McEvoy, …, F. W. Dahlquist. 1996. Phosphotransfer and CheY-binding domains of the histidine autokinase CheA are joined by a flexible linker. *Biochemistry.* 35:433–443.
22. Shimizu, T. S., N. Le Novère, …, D. Bray. 2000. Molecular model of a lattice of signaling proteins involved in bacterial chemotaxis. *Nat. Cell Biol.* 2:792–796.
23. Wuichet, K., R. P. Alexander, and I. B. Zhulin. 2007. Comparative genomic and protein sequence analyses of a complex system controlling bacterial chemotaxis. *Methods Enzymol.* 422:1–31.
24. Zhao, J. H., and J. S. Parkinson. 2006. Mutational analysis of the chemoreceptor-coupling domain of the *Escherichia coli* chemotaxis signaling kinase CheA. *J. Bacteriol.* 188:3299–3307.
25. Hamel, D. J., H. Zhou, …, F. W. Dahlquist. 2006. Chemical-shift-perturbation mapping of the phosphotransfer and catalytic domain interaction in the histidine autokinase CheA from *Thermotoga maritima*. *Biochemistry.* 45:9509–9517.
26. Bhatnagar, J., P. P. Borbat, …, B. R. Crane. 2010. Structure of the ternary complex formed by a chemotaxis receptor signaling domain, the CheA histidine kinase, and the coupling protein CheW as determined by pulsed dipolar ESR spectroscopy. *Biochemistry.* 49:3824–3841.
27. Griswold, I. J., H. Zhou, …, F. W. Dahlquist. 2002. The solution structure and interactions of CheW from *Thermotoga maritima*. *Nat. Struct. Biol.* 9:121–125.
28. Miller, A. S., S. C. Kohout, …, J. J. Falke. 2006. CheA kinase of bacterial chemotaxis: chemical mapping of four essential docking sites. *Biochemistry.* 45:8699–8711.
29. Zhou, H., and F. W. Dahlquist. 1997. Phosphotransfer site of the chemotaxis-specific protein kinase CheA as revealed by NMR. *Biochemistry.* 36:699–710.
30. Underbakke, E. S., Y. M. Zhu, and L. L. Kiessling. 2011. Protein footprinting in a complex milieu: identifying the interaction surfaces of the chemotaxis adaptor protein CheW. *J. Mol. Biol.* 409:483–495.
31. Borbat, P. P., and J. H. Freed. 2007. Measuring distances by pulsed dipolar ESR spectroscopy: spin-labeled histidine kinases. *Methods Enzymol.* 423:52–116.
32. Jeschke, G., and Y. Polyhach. 2007. Distance measurements on spin-labeled biomacromolecules by pulsed electron paramagnetic resonance. *Phys. Chem. Chem. Phys.* 9:1895–1910.
33. Schiemann, O., and T. F. Prisner. 2007. Long-range distance determinations in biomacromolecules by EPR spectroscopy. *Q. Rev. Biophys.* 40:1–53.
34. Borbat, P. P., and J. H. Freed. 2000. Double-quantum ESR and distance measurements. *In* Distance Measurements in Biological Systems by EPR, *Vol. 19*. L. J. Berliner, G. R. Eaton, and S. S. Eaton, editors. Kluwer Academic/Plenum Publishers, New York. 383–459.
35. Milov, A. D., A. G. Maryasov, and Y. D. Tsvetkov. 1998. Pulsed electron double resonance (PELDOR) and its applications in free-radicals research. *Appl. Magn. Reson.* 15:107–143.
36. Jeschke, G. 2002. Distance measurements in the nanometer range by pulse EPR. *Chem. Phys. Chem.* 3:927–932.
37. Borbat, P. P., and J. H. Freed. 1999. Multiple-quantum ESR and distance measurements. *Chem. Phys. Lett.* 313:145–154.
38. Milov, A. D., A. B. Ponomarev, and Y. D. Tsvetkov. 1984. Electron-electron double resonance in electron spin echo: model biradical systems and the sensitized photolysis of decalin. *Chem. Phys. Lett.* 110:67–72.
39. Schiemann, O., P. Cekan, …, S. T. Sigurdsson. 2009. Relative orientation of rigid nitroxides by PELDOR: beyond distance measurements in nucleic acids. *Angew. Chem. Int. Ed. Engl.* 48:3292–3295.
40. Chandrasekhar, S. 1943. Stochastic problems in physics and astronomy. *Rev. Modern Phys.* 15:1–89.
41. Jeschke, G., M. Pannier, …, H. W. Spiess. 2000. Dipolar spectroscopy and spin alignment in electron paramagnetic resonance. *Chem. Phys. Lett.* 331:243–252.
42. Milov, A. D., and Y. D. Tsvetkov. 2000. Charge effect on relative distance distribution of Fremy's radical ions in frozen glassy solution studied by PELDOR. *Appl. Magn. Reson.* 18:217–226.

43. Upadhyay, A. K., P. P. Borbat, …, D. E. Edmondson. 2008. Determination of the oligomeric states of human and rat monoamine oxidases in the outer mitochondrial membrane and octyl β-D-glucopyranoside micelles using pulsed dipolar electron spin resonance spectroscopy. *Biochemistry.* 47:1554–1566.

44. Chiang, Y. W., P. P. Borbat, and J. H. Freed. 2005. The determination of pair distance distributions by pulsed ESR using Tikhonov regularization. *J. Magn. Reson.* 172:279–295.

45. Chiang, Y. W., P. P. Borbat, and J. H. Freed. 2005. Maximum entropy: a complement to Tikhonov regularization for determination of pair distance distributions by pulsed ESR. *J. Magn. Res.* 177: 184–196.

46. Pollard, A. M., A. M. Bilwes, and B. R. Crane. 2009. The structure of a soluble chemoreceptor suggests a mechanism for propagating conformational signals. *Biochemistry.* 48:1936–1944.

47. Bass, R. B., S. L. Butler, …, J. J. Falke. 2007. Use of site-directed cysteine and disulfide chemistry to probe protein structure and dynamics: applications to soluble and transmembrane receptors of bacterial chemotaxis. *Methods Enzymol.* 423:25–51.

48. Gegner, J. A., and F. W. Dahlquist. 1991. Signal transduction in bacteria: CheW forms a reversible complex with the protein kinase CheA. *Proc. Natl. Acad. Sci. USA.* 88:750–754.

49. Surette, M. G., M. Levit, …, J. B. Stock. 1996. Dimerization is required for the activity of the protein histidine kinase CheA that mediates signal transduction in bacterial chemotaxis. *J. Biol. Chem.* 271: 939–945.

50. Park, S. Y., C. M. Quezada, …, B. R. Crane. 2004. Subunit exchange by CheA histidine kinases from the mesophile *Escherichia coli* and the thermophile *Thermotoga maritima*. *Biochemistry.* 43:2228–2240.

51. Georgieva, E. R., A. S. Roy, …, J. H. Freed. 2012. Effect of freezing conditions on distances and their distributions derived from double electron electron resonance (DEER): a study of doubly-spin-labeled T4 lysozyme. *J. Mag. Res.* 10.1016/j.jmr.2012.01.04.

52. Hess, J. F., R. B. Bourret, and M. I. Simon. 1991. Phosphorylation assays for proteins of the two-component regulatory system controlling chemotaxis in *Escherichia coli*. *Methods Enzymol.* 200:188–204.

53. Gegner, J. A., D. R. Graham, …, F. W. Dahlquist. 1992. Assembly of an MCP receptor, CheW, and kinase CheA complex in the bacterial chemotaxis signal transduction pathway. *Cell.* 70:975–982.

54. Bode, B. E., D. Margraf, …, O. Schiemann. 2007. Counting the monomers in nanometer-sized oligomers by pulsed electron-electron double resonance. *J. Am. Chem. Soc.* 129:6736–6745.

55. Milov, A. D., R. I. Samoilova, …, J. Raap. 2009. Structure of self-aggregated alamethicin in ePC membranes detected by pulsed electron-electron double resonance and electron spin echo envelope modulation spectroscopies. *Biophys. J.* 96:3197–3209.

56. Tong, J. S., P. P. Borbat, …, Y. K. Shin. 2009. A scissors mechanism for stimulation of SNARE-mediated lipid mixing by cholesterol. *Proc. Natl. Acad. Sci. USA.* 106:5141–5146.